

Citation for published version:

S. Kaviraj, et al., "Radio AGN in spiral galaxies", *Monthly Notices of the Royal Astronomical Society*, Vol 454(2), October 2015.

DOI:

<https://doi.org/10.1093/mnras/stv1957>

Document Version:

This is the Published Version.

Copyright and Reuse:

© 2015 The Authors Published by Oxford University Press on behalf of the Royal Astronomical Society.

Content in the UH Research Archive is made available for personal research, educational, or non-commercial purposes only. Unless otherwise stated all content is protected by copyright, and in the absence of an open licence permissions for further reuse of content should be sought from the publisher, author or other copyright holder.

Enquiries

If you believe this document infringes copyright, please contact the Research & Scholarly Communications Team at rsc@herts.ac.uk

Radio AGN in spiral galaxies

Sugata Kaviraj,¹★ Stanislav S. Shabala,² Adam T. Deller³ and Enno Middelberg⁴

¹Centre for Astrophysics Research, University of Hertfordshire, College Lane, Hatfield, Herts AL10 9AB, UK

²School of Mathematics and Physics, University of Tasmania, Private Bag 37, Hobart, TAS 7001, Australia

³ASTRON, The Netherlands Institute for Radio Astronomy, Postbus 2, NL-7990 AA, Dwingeloo, The Netherlands

⁴Astronomisches Institut der Ruhr-Universität Bochum, Universitätsstraße 150, D-44801 Bochum, Germany

Accepted 2015 August 20. Received 2015 July 13; in original form 2014 December 15

ABSTRACT

Radio AGN in the nearby Universe are more likely to be found in galaxies with early-type morphology, the detection rate in spiral or late-type galaxies (LTGs) being around an order of magnitude lower. We combine the mJy Imaging VLBA Exploration at 20 cm (mJIVE-20) survey with the Sloan Digital Sky Survey, to study the relatively rare population of AGN in LTGs that have nuclear radio luminosities similar to that in their early-type counterparts. The LTG AGN population is preferentially hosted by galaxies that have high stellar masses ($M_* > 10^{10.8} M_\odot$), red colours and low star formation rates, with little dependence on the detailed morphology or local environment of the host LTG. The merger fraction in the LTG AGN is ~ 4 times higher than that in the general LTG population, indicating that merging is an important trigger for radio AGN in these systems. The red colours of our systems extend recent work which indicates that merger-triggered AGN in the nearby Universe appear *after* the peak of the associated starburst, implying that they do not strongly regulate star formation. Finally, we find that in systems where parsec-scale jets are clearly observed in our very long baseline interferometry images, the jets are perpendicular to the major axis of the galaxy, indicating strong alignment between the accretion disc and the host galaxy stellar disc.

Key words: galaxies: active – galaxies: evolution – galaxies: formation – galaxies: interactions – galaxies: spiral.

1 INTRODUCTION

Radio AGN are a cornerstone of modern galaxy formation models, the current consensus favouring a paradigm in which AGN feedback regulates star formation and shapes fundamental features of the galaxy population like their distribution of colours and luminosities (e.g. Hatton et al. 2003; Croton et al. 2006; Somerville et al. 2012). Observational work indicates that radio AGN, at least in the local Universe, are more common in early-type galaxies (ETGs). For example, Kaviraj et al. (2015) have shown that the detection rate in very long baseline interferometry (VLBI) observations for ETGs is around an order of magnitude higher than in their late-type counterparts, when galaxy stellar mass is controlled for – this is qualitatively similar to the findings of other studies in the literature (e.g. Ledlow et al. 2001; Sadler et al. 2014). Radio AGN are, therefore, comparatively rare in late-type galaxies (LTGs) compared to their early-type counterparts, with relatively few examples having been studied in the past literature (e.g. Ekers et al. 1978; Ulvestad & Wilson 1984; Edelson 1987; Norris, Allen & Roche 1988; Norris

et al. 1990; Ledlow, Owen & Keel 1998; Morganti et al. 2001; Keel et al. 2006; Zhou et al. 2007; Yuan et al. 2008; Gliozzi et al. 2010; Inskip et al. 2010; Norris et al. 2012; Mao et al. 2014). In particular, Sadler et al. (1995) have performed a detailed study of the properties of parsec-scale radio cores in local early and LTGs and studied the differences between the hosts of radio AGN in galaxies of different morphological types.

The study of radio AGN in LTGs is desirable not just because they are rare, but also because they may hold clues to the behaviour of radio jets in disc environments. While this is uncommon at low redshift, the bulk of the stellar and black hole mass in today’s Universe was created at $z \sim 2$ (e.g. Madau, Pozzetti & Dickinson 1998; Hopkins & Beacom 2006), an epoch at which both star formation (e.g. Kaviraj et al. 2013) and black hole growth (e.g. Kocevski et al. 2012; Schawinski et al. 2012) were predominantly hosted by LTGs. The connection between the black hole and a disc-like host system was therefore common around the epoch of peak cosmic star formation, making radio AGN in nearby LTGs useful laboratories for exploring this connection.

Given their relative rarity, a statistical study of radio AGN in LTGs requires a combination of survey-scale radio data (for the detection of large numbers of radio AGN) and high-resolution optical imaging

* E-mail: s.kaviraj@herts.ac.uk

(for accurate determination of galaxy morphologies). In this study, we combine mJIVE-20 (Deller & Middelberg 2014; see section 2.1) with optical imaging and spectro-photometry from the Sloan Digital Sky Survey (SDSS; Abazajian et al. 2009), to study radio AGN in the nearby ($z < 0.3$) LTG population.

The high resolution of VLBI enables unambiguous identification of AGN, because the $> 10^6$ K temperatures required for a detection cannot be achieved via star formation alone and requires non-thermal sources like supernova remnants (SNRs), radio supernovae (SNe) or AGN. Only in the very local Universe and in vigorous starbursting systems can clusters of luminous SNe and SNRs reach sufficiently high luminosities to be visible in a (shallow) VLBI observation. In the extreme example of Arp 220, which has a star formation rate of several hundred solar masses per year (e.g. Iwasawa et al. 2005; Baan 2007), the brightest VLBI-scale sources reach a peak VLBI flux density of ~ 1 mJy beam $^{-1}$ (Lonsdale et al. 2006). As we indicate below, our sample consists of sources that are both more distant and have lower star formation rates than Arp 220, making it extremely unlikely that the relatively shallow mJIVE-20 observations (with a detection limit of ~ 1 mJy) would detect anything other than an AGN in our target sample.

While in lower resolution surveys like FIRST and NVSS, AGN identification requires the detection of excess radio flux beyond what is expected from star formation (biasing samples towards AGN that dominate the star formation), or a dense gas environment which the jet works against to produce detectable radio lobes (introducing a bias against AGN in LTGs, which do not typically host extensive hot gas haloes), VLBI is capable of identifying AGN irrespective of the host galaxy properties (e.g. star formation rate, environment etc.). Some limitations of VLBI are worth noting here. Of the total radio emission generated by AGN activity, only a fraction will typically be confined to the parsec-scale core/jet at the site of the central black hole, as extended radio lobes will often be present – hence, the compact flux fraction can be influenced by the surrounding galactic environment. The prominence of the compact core depends on the source age and orientation (which can result in Doppler boosting or deboosting of the compact emission). Finally, hotspots at the site of the jet interaction with the interstellar medium (as are seen in compact symmetric objects; Phillips & Mutel 1982; Wilkinson et al. 1994) may also be compact enough to be visible in VLBI observations, so that, although VLBI detections can unambiguously be associated with AGN, they cannot in every case be associated with AGN cores. However, this last case can usually be distinguished on the basis of morphology. Nevertheless, the unambiguity in the identification of AGN activity makes VLBI data from mJIVE-20 the ideal route for studying the local AGN population that inhabits LTGs.

Here, we identify our spiral AGN hosts via direct visual inspection of the SDSS colour images of mJIVE-20 detections. We then study their physical properties, derived from SDSS spectro-photometric data, to explore the conditions that make it likely for LTGs to host AGN. This is the first study where survey-scale VLBI data is combined with visual inspection of galaxy images to study a *morphologically selected* sample of LTGs that host radio AGN. The sections below are organized as follows. In Section 2, we briefly describe the mJIVE-20 and SDSS data that underpin this study. In Section 3, we compare the properties of LTGs that host radio AGN with those of the general LTG population. We discuss and summarize our findings in Section 4. Throughout, we employ the WMAP7 cosmological parameters (Komatsu et al. 2011) and photometry in the AB system (Oke & Gunn 1983).

2 DATA

2.1 Radio VLBI data

mJIVE-20 is an ongoing survey using the VLBA that is systematically observing objects detected by the FIRST radio survey. mJIVE-20 uses short segments scheduled in bad weather or with a reduced number of antennas during which no highly rated VLBA science projects can be scheduled. The survey has targeted $\sim 25\,000$ FIRST sources to date, with ~ 5000 VLBI detections. While the sensitivity and resolution of mJIVE-20 varies between different fields, the median detection threshold is 1.2 mJy beam $^{-1}$ and the typical beam size is 6×17 milliarcsec. This corresponds to a detection sensitivity of $\sim 10^7$ K (the variation between fields is around a factor of 2). We refer readers to Deller & Middelberg (2014) for further details of the survey.

2.2 SDSS data

The mJIVE-20 targets are cross-matched with the latest data release of the SDSS (Abazajian et al. 2009). Following Shabala et al. (2008), we use a matching radius of 2 arcsec for the radio–optical matching, which yields high (96 per cent) completeness and low (0.3 per cent) contamination. Since morphological classification and the identification of morphological disturbances will be an important part of our study, we restrict ourselves to SDSS galaxies that have photometric or spectroscopic redshifts less than 0.3. This yields 437 SDSS galaxies with mJIVE-20 detections in this redshift range. The entire sample is visually classified, via the SDSS colour images, to separate ETGs from LTGs. For each galaxy, we also note the presence of morphological disturbances, indicating that the galaxy has had a recent merger or interaction.

This visual classification yields 29 VLBI-detected LTGs. Fig. 1 presents examples of these systems. Note that the VLBI-detected LTGs span the full spectrum of spiral morphologies seen on the Hubble sequence (e.g. Hubble 1926; de Vaucouleurs 1959), from systems that have reasonably prominent bulges to those that are clearly dominated by discs. It is also worth noting that the VLBI-detected LTGs show a high incidence of morphological disturbances, suggesting that these systems have undergone recent mergers (we return to this point in our analysis below).

Out of the 29 VLBI-detected LTGs, 11 have SDSS spectra and therefore spectroscopic redshifts. Our analysis below is restricted to these objects, since quantities like absolute magnitudes, stellar masses and local environments require an accurate measurement of redshift. For this spectroscopically detected subsample, magnitudes are K-corrected using the `KCORRECT` code of Blanton & Roweis (2007) and published stellar masses, star formation rates and emission-line classes are extracted from the latest version of the publicly available MPA-JHU value-added SDSS catalogue (Kauffmann et al. 2003; Brinchmann et al. 2004; Tremonti et al. 2004).¹

The emission-line class of each galaxy has been calculated through a standard line-ratio analysis (Kauffmann et al. 2003, see also Baldwin, Phillips & Terlevich 1981; Veilleux & Osterbrock 1987; Kewley et al. 2006), using the measured values of $[\text{N II}]/\text{H}\alpha$ and $[\text{O III}]/\text{H}\beta$. Objects in which all four emission lines are detected with a signal-to-noise (S/N) ratio greater than 3 are classified in the MPA-JHU catalogue as either ‘star-forming’, ‘low S/N star-forming’, ‘composite’, ‘Seyfert’ or ‘LINER’, depending on their

¹ <http://www.mpa-garching.mpg.de/SDSS/DR7/>

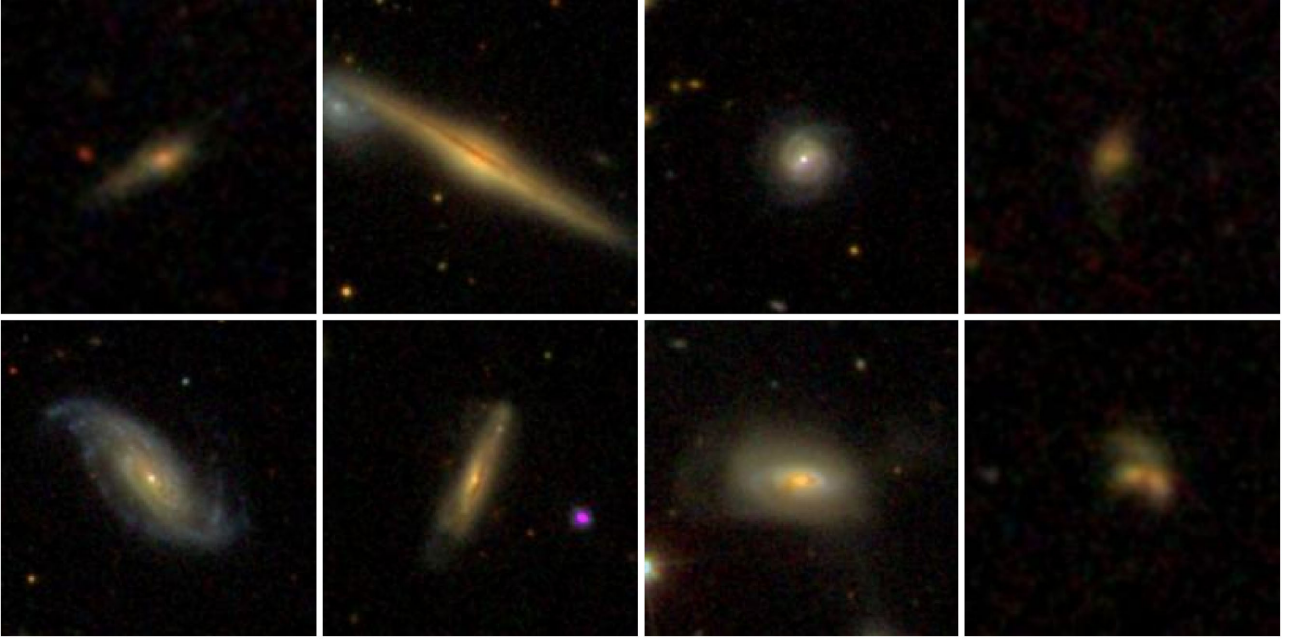


Figure 1. SDSS colour images of a sample of VLBI-detected spiral galaxies that underpin this study.

location in the $[\text{N II}]/\text{H}\alpha$ versus $[\text{O III}]/\text{H}\beta$ diagram. Galaxies without a detection in all four lines are classified as ‘quiescent’ (Kauffmann et al. 2003).

Finally, the local environments of these spectroscopically detected galaxies are extracted from the group catalogue of Yang et al. (2007), who use a halo-based group finder to separate the SDSS into over 300 000 structures with a broad dynamic range, from rich clusters to isolated galaxies. Yang et al. (2007) estimate the host dark matter halo masses of individual SDSS galaxies, which are related to the traditional classifications of environment (‘field’, ‘group’ and ‘cluster’). Cluster-sized haloes typically have masses greater than $10^{14} M_{\odot}$, while group-sized haloes have masses between 10^{13} and $10^{14} M_{\odot}$ (Binney & Tremaine 1987). Table 1 lists the galaxies that underpin this study, along with their basic properties.

3 RADIO AGN IN SPIRAL GALAXIES

Given that VLBI detections are possible in rare, intensely starbursting galaxies like Arp 220, we first check whether our spiral AGN hosts are consistent with an Arp 220-like starburst. The VLBI-detected LTGs have SFRs (Fig. 5) that are significantly lower than that in Arp 220, which has an SFR of several hundred solar masses per year (e.g. Iwasawa et al. 2005; Baan 2007). They also lie much further away than Arp 220, which has a redshift of 0.018 (Fig. 3). This indicates that the VLBI radio fluxes in these systems are not driven by star formation in an Arp 220-like system. This conclusion is consistent with the SDSS images of these galaxies (see Fig. 1), which indicate that most of these objects are not dusty major-merger remnants like Arp 220, but are normal massive galaxies with a disc-like morphology.

A further test for contamination by sources such as radio SNe can be made by exploring the positional offsets between the VLBI source and the optical centre of the galaxy. While very young radio SNe could exhibit brightness temperatures around 10^7 K for several years after the initial explosion (e.g. Weiler et al. 2007), the

radio emission from such objects would be offset from the optical centre of the galaxy. However, the positional offsets between the VLBI and optical detections in our LTGs (see Fig. 2) are within the SDSS resolution of 1.5 arcsec, indicating that the VLBI radio sources coincide well with the optical centres of our galaxies and are, therefore, unlikely to be radio SNe. In summary, therefore, it seems reasonable to conclude that the radio emission in our LTGs is driven by central AGN.

3.1 Physical properties of spiral AGN hosts

We begin our analysis by studying the physical properties of the LTGs that host radio AGN. Fig. 3 indicates that the radio AGN in our LTG sample span a similar range in masses and nuclear radio luminosities as their early-type counterparts. We are, therefore, studying radio AGN in spirals that broadly share the same physical properties as the more commonly found radio AGN in early-type systems in the same stellar mass and redshift ranges.

In our subsequent analysis, we compare the physical properties of our VLBI-detected LTGs to two different populations of LTGs. Since most of our VLBI-detected LTGs have stellar masses greater than $M_{*} \sim 10^{10.8} M_{\odot}$ (see Fig. 4) and have been restricted to $z < 0.3$, we restrict all other samples to these stellar mass and redshift ranges. The first population is the sample of 77 LTGs that are mJIVE-20 targets but are undetected (we refer to these galaxies as ‘VLBI-undetected LTGs’). Since the VLBI-undetected LTGs are, by construction, detected by FIRST, we also define a ‘control sample’ of LTGs that are not radio detected. To construct this control sample we select a random ~ 230 spiral galaxies from the SDSS via an identical visual inspection as was performed on the mJIVE-20 targets.

Fig. 4 presents the stellar mass and redshift properties of each of these LTG populations. It is worth noting that the VLBI-detected spirals generally lie towards the upper envelope of the mass-redshift space. KS-tests between the mass distributions of the VLBI-detected

Table 1. VLBI-detected LTGs. The analysis presented in this paper is based on galaxies that have spectroscopic redshifts and data from the SDSS (top section of the table). LTGs that are not part of this study due to the lack of spectroscopic data are also listed for completeness. (1) ID (2) Spectroscopic redshift (3) mJIVE RA (4) mJIVE DEC (5) log of stellar mass [M_{\odot}] (6) log L (mJIVE) [W Hz^{-1}] (7) log L (FIRST) [W Hz^{-1}] (8) $u - r$ colour (9) log SFR [$M_{\odot} \text{ yr}^{-1}$].

ID	z	RA	DEC	log M_*	log L (mJIVE)	log L (FIRST)	$u - r$	log SFR
1	0.129	45.1952	-0.0323	11.425	23.412	23.462	2.873	-0.323
2	0.021	153.0151	23.0857	10.830	22.192	22.365	2.531	-0.184
3	0.141	158.8169	39.8802	11.606	23.571	23.656	2.603	-0.516
4	0.130	165.4924	12.0920	11.248	22.887	22.902	2.253	0.338
5	0.028	166.3412	38.2338	10.355	21.879	22.671	1.823	0.967
6	0.238	177.8164	23.8274	11.026	23.109	23.404	1.478	1.425
7	0.028	196.5185	55.6560	11.178	22.261	22.326	2.569	-0.846
8	0.034	217.4105	10.5841	10.649	21.617	22.015	1.857	0.456
9	0.237	218.8011	42.5170	11.620	23.557	23.743	2.591	0.478
10	0.029	222.8721	9.3350	10.956	21.243	22.815	2.399	1.407
11	0.071	253.8005	39.1894	11.252	22.990	23.347	2.476	0.507
12	-	116.8725	25.5233					
13	-	125.5146	56.0504					
14	-	154.0926	61.7083					
15	-	158.6608	39.6412					
16	-	165.7969	27.9726					
17	-	179.4875	16.6526					
18	-	181.7136	28.2590					
19	-	186.1500	39.3833					
20	-	197.1664	12.0113					
21	-	197.8753	32.6417					
22	-	202.8411	31.8555					
23	-	211.4069	56.3313					
24	-	212.3108	2.5162					
25	-	216.7148	36.6481					
26	-	217.4980	53.7178					
27	-	237.5461	5.3634					
28	-	240.8432	29.8731					
29	-	329.9206	3.4211					

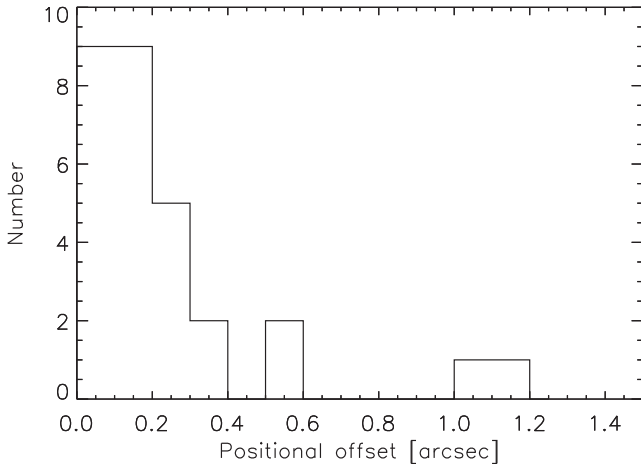


Figure 2. Positional offsets between the VLBI sources and the optical centres of our galaxies.

LTGs compared to the VLBI-undetected and control LTGs yield p -values of $\sim 10^{-5}$ and $\sim 10^{-4}$, respectively, indicating that the spirals with AGN are likely to be drawn from different parent distributions. The offset towards higher masses in the VLBI-detected systems is plausibly due to larger galaxies having bigger black holes (Gültekin et al. 2009) which, in turn, produce more powerful jets (e.g. Shabala et al. 2008). It is worth noting here that, given the small number of galaxies in our VLBI-detected LTG sample, it is not pos-

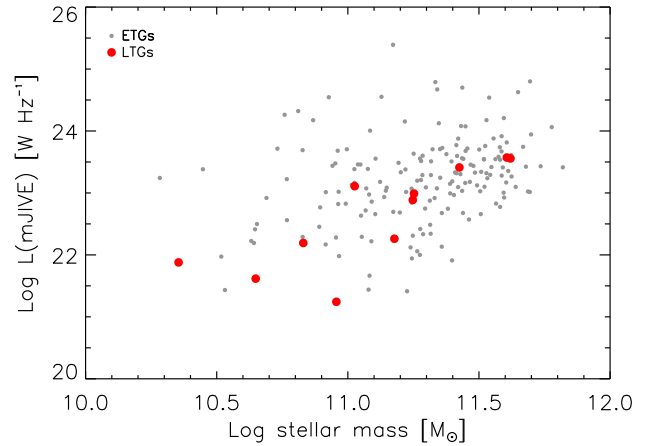


Figure 3. mJIVE-20 radio luminosities of VLBI-detected spirals compared to that of their early-type counterparts in the same stellar mass and redshift range. The spirals span the same range in mass and nuclear radio luminosity as their early-type counterparts, although the median values (on a log scale) for the spirals [11.18 (mass) and 22.99 (radio luminosity)] are slightly smaller than for their early-type counterparts [11.31 (mass) and 23.29 (radio luminosity)].

sible to construct a control sample that has a matched distribution in redshift and mass, as one would ideally want. As a result, properties of the control sample – such as its median redshift – are only indicative. Nevertheless, we note that, while several of our VLBI-detected

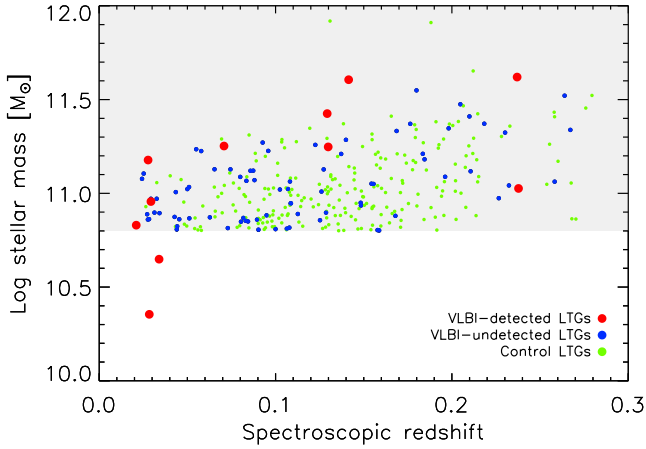


Figure 4. Stellar mass versus redshift of VLBI-detected (red) and VLBI-undetected (blue) and control (green) spiral galaxies. The shaded region indicates the stellar mass range considered in our analysis in Section 3.

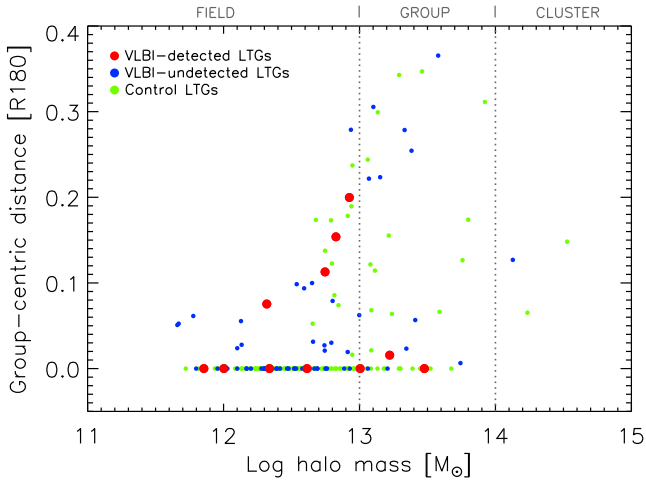


Figure 5. Halo mass versus group-centric radii of VLBI-detected (red), VLBI-undetected (blue) and control (green) spiral galaxies.

LTGs lie towards the lower end of our redshift range, they would still be detectable if they were placed at the median redshift of the control sample ($z \sim 0.12$).

Fig. 5 shows the environments of the spiral AGN hosts compared to that of their VLBI-undetected and control counterparts. Paired (i.e. 2D) KS-tests in the halo mass – group centric radius plane between the VLBI-detected LTGs and their VLBI-undetected and control counterparts yield p -values of 0.06 and 0.01, respectively. Thus, while the environments of the VLBI-detected and undetected populations are likely to be similar, there is a hint that the VLBI-detected LTGs are somewhat different from the control LTGs. The difference is probably driven by the fact that the VLBI detections appear to avoid the highest halo masses compared to the control sample. However, local environment, on the whole, appears not to play a major role in determining the presence of radio AGN in LTGs.

The VLBI-detected spirals generally show redder $(u-r)$ colours and correspondingly lower SFRs than the undetected and control populations (Fig. 6). KS-tests between the VLBI-detected and control LTGs in either of these quantities yield very low p -values ($< 10^{-3}$), indicating that the spiral AGN hosts are likely to be different from the general LTG population in these proper-

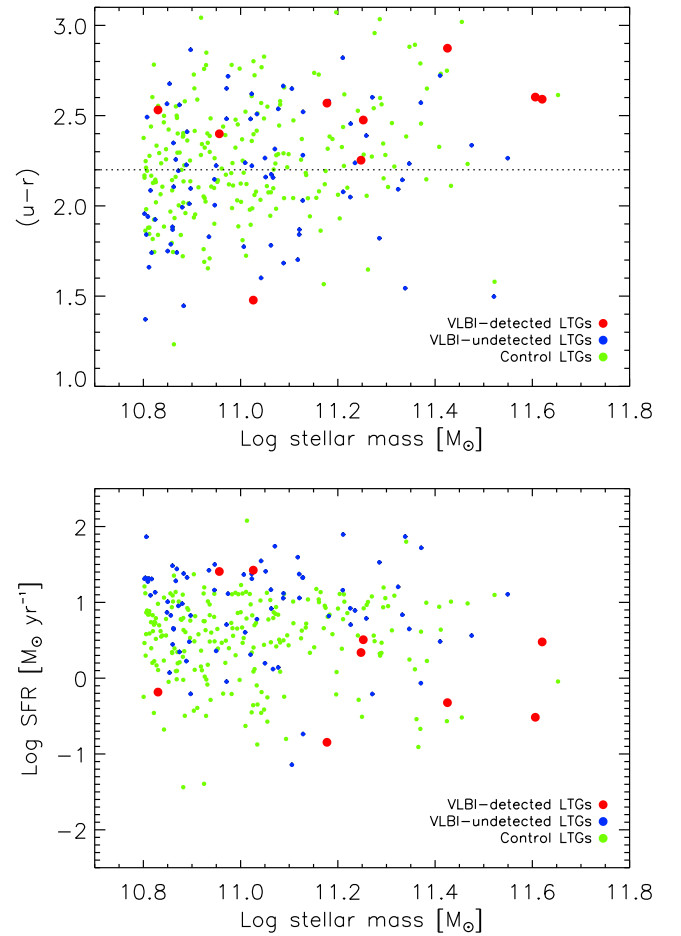


Figure 6. $(u-r)$ (top) and SFR (bottom) versus stellar mass for the VLBI-detected (red), VLBI-undetected (blue) and control (green) spiral galaxies. The dotted line in the top panel indicates the demarcation between the red sequence and the blue cloud (e.g. Strateva et al. 2001).

ties. ~ 90 per cent of the VLBI-detected LTGs are on the red sequence, compared to ~ 50 per cent of the VLBI-undetected sample and ~ 60 per cent of the control LTG sample (column 1 in Table 2). In a similar vein, only two out of the nine VLBI-detected LTGs lie on the SFR-mass parameter space defined by the bulk of the control and VLBI-undetected populations.²

As has been noted in the literature (e.g. Greene et al. 2013), the mechanism that dissipates angular momentum and allows gas to accrete on to the central black hole remains unclear. The removal of angular momentum could take place as a result of processes such as merging (e.g. Sanders et al. 1988), or via circumnuclear structures such as bars (e.g. Maciejewski et al. 2002; Kim, Seo & Kim 2012) or nuclear spirals (e.g. Englmaier & Shlosman 2000; Martini et al. 2003; Davies et al. 2009). Column 2 in Table 2 presents merger fractions in our three LTG samples. The VLBI-detected LTGs show the highest merger fraction (~ 50 per cent), which is around a factor of 2 higher than that in their undetected counterparts and around a factor of 4 higher than that in the control LTGs. While other processes that drive the dissipation of angular momentum cannot be completely ruled out, the remarkably high merger fraction in the VLBI-detected

² It is worth noting here that some of our spiral AGN are on the star formation main sequence, illustrating the utility of VLBI in being able to detect AGN regardless of the level of star formation activity in the host system.

Table 2. Comparison of the properties of VLBI-detected, VLBI-undetected and control LTGs. Columns are as follows. (1) Galaxy number fraction on the red sequence, defined as $u - r > 2.2$ (2) The fraction of galaxies that are currently merging or are post-mergers (3–8) Fraction of galaxies in each BPT classification class (star-forming [SF]), low S/N star forming, composites [Cp], Seyferts [Sy], LINERs [LI] and quiescent [Qs]).

	Red	Mgr	SF	Low S/N SF	Cp	Sy	LI	Qs
VLBI-detected LTGs	0.90 ^(0.35)	0.53 ^(0.21)	0.08 ^(0.07)	0.08 ^(0.07)	0.23 ^(0.17)	0.30 ^(0.18)	0.23 ^(0.17)	0.08 ^(0.07)
VLBI-undetected LTGs	0.48 ^(0.16)	0.28 ^(0.06)	0.14 ^(0.04)	0.07 ^(0.03)	0.41 ^(0.08)	0.29 ^(0.06)	0.05 ^(0.02)	0.02 ^(0.01)
Control LTGs	0.62 ^(0.06)	0.16 ^(0.02)	0.12 ^(0.02)	0.41 ^(0.04)	0.12 ^(0.02)	0.06 ^(0.02)	0.19 ^(0.03)	0.10 ^(0.02)

spirals suggests that mergers are likely to play a significant role in triggering radio AGN in spiral hosts. It is worth noting that the SDSS images that form the basis of the visual inspection and the identification of morphological disturbances are relatively shallow, with standard exposure times of 54 s. As mentioned in the recent literature (e.g. Kaviraj 2010), merger fractions derived from such images are, therefore, strictly lower limits. It is possible (and likely) that a much larger fraction of the VLBI-detected LTGs carry morphological disturbances, that are invisible in the shallow standard-depth SDSS images. Note that, although our galaxy sample spans the redshift range $0 < z < 0.3$, our ability to identify these relatively faint tidal features remains stable across this redshift range. This is because, since apparent brightness and apparent area both follow an inverse square relation, the surface brightness of tidal features does not change significantly with increasing redshift [at least at low redshift where cosmological surface brightness dimming is a very slow function of redshift (see e.g. van Dokkum 2005)].

A merger trigger for the AGN appears to be supported by the emission-line analysis of our sample (Fig. 7 and columns 4–8 in Table 2). The BPT analysis suggests an increasing fraction of optical emission-line AGN as we transition from the control LTG sample to the VLBI-detected population. While ~ 37 per cent of the control sample show evidence for an optical AGN (i.e. systems classified as composite, Seyferts or LINERs), the corresponding fraction in the VLBI-detected population is ~ 76 per cent. It is worth noting that in ETGs, some LINERs may not be driven by AGN (e.g. Sarzi et al. 2010). Even if this was also the case in LTGs and the LINERs were removed from this argument, the VLBI-detected spirals still show a surfeit of optical AGN of around a factor of 3. This high fraction of optical AGN appears consistent with a radiatively efficient cold-mode-type accretion, which might be expected if the gas has been accreted via a merger, as seems to be the case for our sample (e.g. Hardcastle, Evans & Croston 2007; Best & Heckman 2012; Shabala et al. 2012). Our results appear consistent with recent work that has suggested a strong connection between merging and the onset of AGN activity at low redshift (e.g. Koss et al. 2010; Ellison et al. 2011; Scott & Kaviraj 2014; Kaviraj et al. 2015), although the role of mergers in triggering AGN may become negligible at high redshift (e.g. Chiaberge & Marconi 2011; Kocevski et al. 2012; Schawinski et al. 2012).

The analysis above indicates that local LTGs that host radio AGN (with luminosities similar to those found in their early-type counterparts) tend to be massive spirals with low SFRs, with mergers being a plausible trigger for the onset of the AGN. It is worth noting that the requirements for LTGs to host radio AGN are akin to those in their early-type counterparts that inhabit similar (low-density) environments i.e. massive galaxies that have red colours and are likely to be involved in a merger (Kaviraj et al. 2015). Nevertheless, the detection rate in early types is almost an order of magnitude higher (Kaviraj et al. 2015). While a thorough investigation is beyond the scope of this particular paper, we speculate on some of the potential reasons for this discrepancy. It is possible that hot gas reservoirs in

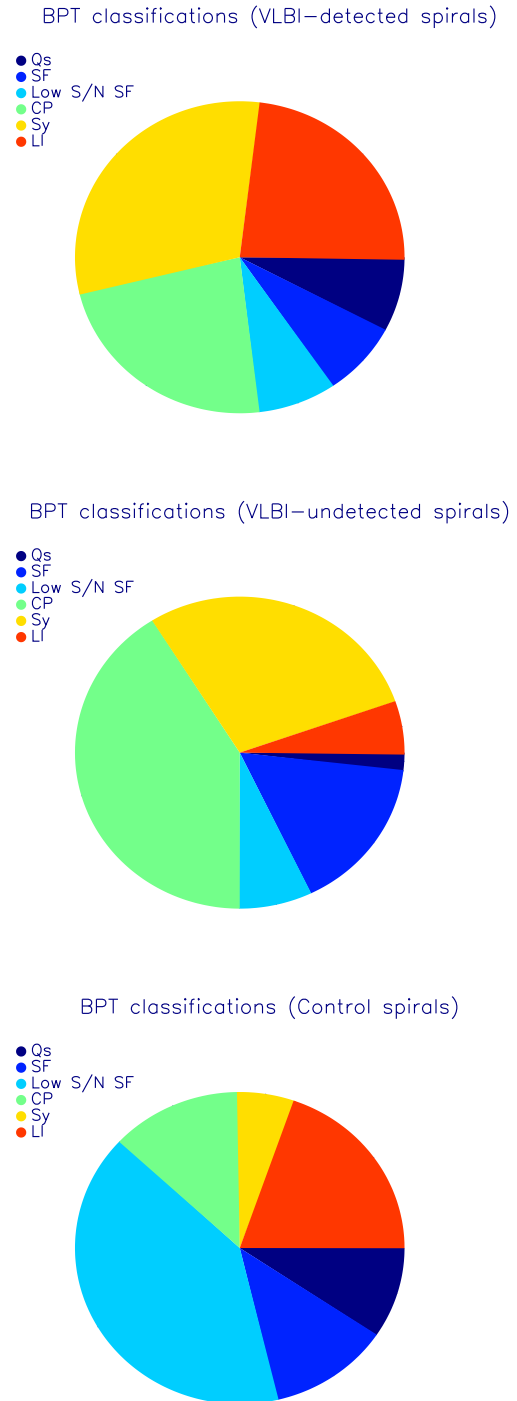


Figure 7. BPT classifications of VLBI-detected (top), VLBI-undetected (middle) and control (bottom) spiral galaxies. The fractions of galaxies in each BPT class are indicated in Table 2.

ETGs could provide an extra source of fuel for the black hole – we note, however, that the Kaviraj et al. (2015) sample does not contain central cluster galaxies where hot gas cooling is expected to play a significant role in AGN triggering (e.g. Tabor & Binney 1993; McNamara & Nulsen 2007; Cattaneo et al. 2009; Fabian 2012). Thus, it is unclear if the observed discrepancy in detection rate can be completely explained solely via this argument. Alternatively (or in addition), black hole masses may trace bulge mass more closely than total galaxy stellar mass, implying that even massive LTGs do not typically have black holes as massive as those in their early-type counterparts. Finally, the ‘spin paradigm’, which postulates that radio jets are launched by rapidly spinning black holes (e.g. Blandford & Znajek 1977; Wilson & Colbert 1995; Sikora, Stawarz & Lasota 2007; Bagchi et al. 2014) that are expected to reside primarily in bulge-dominated galaxies, may also play a leading role in explaining the surfeit of radio AGN in early-type systems compared to their late-type counterparts.

3.2 Implications for AGN feedback in spiral AGN hosts

The recent literature indicates that, in low-density environments in the *nearby* Universe, AGN overwhelmingly avoid systems that are in the blue cloud i.e. that are experiencing the peak of their star formation episode (e.g. Schawinski et al. 2007; Wild, Heckman & Charlot 2010; Kaviraj et al. 2011; Carpineti et al. 2012; Kaviraj 2014). Radio AGN in early types, for example, cluster strongly on the red sequence, where star formation rates have declined significantly (Kaviraj et al. 2015). Given that typical AGN lifetimes (a few times 10^7 yr; e.g. Shabala et al. 2008) are much shorter than the transit time from blue cloud to red sequence, this suggests a time lag between the onset of star formation and the triggering of AGN. Interestingly, this time lag shows no dependence on the intensity of star formation (and therefore the gas fraction) in the host system and is observed across the entire spectrum of star formation activity, from intensely starbursting luminous infrared galaxies (Kaviraj 2009) to the relatively weakly star-forming early-type systems (e.g. Wild et al. 2010; Shabala et al. 2012). The implication of this time delay is that the AGN typically does not couple to the host’s gas reservoir during the main starburst phase, thus reducing its ability to strongly regulate the stellar mass growth.

Our study reinforces this picture, by extending these results to spiral AGN hosts. In a similar vein to what is found in ETGs, radio AGN in the nearby LTG population preferentially inhabit systems on the red sequence that have low SFRs. Unless the typical AGN lifetime (i.e. the duration of the ‘on’ phase) is significantly longer in LTGs compared to their early-type counterparts, the radio AGN in our spiral hosts are also likely to have been triggered after the peak of the star formation activity has elapsed in these systems, limiting their ability to impart feedback on the gas reservoir. Taken together with the recent literature, our results indicate that the time delay between the onset of merger-driven star formation and the subsequent triggering of AGN is likely to be a ubiquitous feature of radio AGN in the nearby Universe.

3.3 Jet orientations in spiral AGN hosts

We conclude this section by exploring the morphology of the jets in our VLBI-detected spirals. Three galaxies in our sample show clear VLBI-scale jets. In Fig. 8, we present the VLBI radio maps of these galaxies, together with their optical SDSS and arcsec-scale radio images from FIRST. In all cases, the VLBI-scale jets are clearly close to being orthogonal to the galaxy disc. Since the jet is

expected to align with the spin axis of the black hole (e.g. McKinney, Tchekhovskoy & Blandford 2013), the orthogonality observed in our galaxies is not unexpected, since co-evolution of the black hole and the host spiral should produce alignment between the black hole’s spin axis and the stellar disc. In such a scenario, one would expect the jet to be orthogonal to the major axis of the spiral galaxy, as is observed in our galaxies.

It is worth recalling that a high fraction (50 per cent +) of our LTG AGN are likely merger remnants. One might expect that galaxy mergers could disrupt the alignment between the black hole spin axis and the stellar disc e.g. due to the coalescence of two similar mass black holes in a major merger. However, it is important to note that the interactions in question here are, by definition, *minor* mergers (i.e. mergers with small satellites), because the discs in our LTG AGN remain intact, contrary to what might be expected in major-merger remnants (e.g. Barnes & Hernquist 1992; Springel, Di Matteo & Hernquist 2005). Our results therefore suggest that minor mergers are unlikely to disrupt the alignment between the black hole spin axis and the stellar disc (which may naturally come about due to secular co-evolution of these two systems).³

Finally, it is worth noting that several authors have studied the relative geometry of galaxy-scale and circumnuclear structures in systems that host AGN. Most recently, Greene et al. (2013) used H₂O megamaser observations to map the circumnuclear discs in seven nearby Seyfert galaxies, and found that while the maser discs are oriented perpendicular to the direction of VLBI-scale radio jets (consistent with jet generation models in which the magnetic field associated with the black hole’s accretion disc determines jet orientation, e.g. McKinney et al. 2013), the maser and galaxy discs did not align in most of their sample. While the reasons for this discrepancy with our results are difficult to probe further using the available data, several causes for such misalignments are possible, including disc warping on parsec scales, subparsec-scale torques from stars in a cusp around the black hole and natural changes in the angular momentum vector of (secularly) infalling gas as it is torqued by the stars (e.g. Maloney, Begelman & Pringle 1996; Pringle 1997; Gammie, Goodman & Ogilvie 2000; Hopkins & Quataert 2010; Greene et al. 2013).

4 SUMMARY AND DISCUSSION

We have combined the mJIVE-20 radio VLBI survey with the SDSS to study the rare population of radio AGN in LTGs that have radio luminosities similar to the more commonly found early-type AGN in the same stellar mass and redshift ranges. As noted in the introduction, the study of radio AGN in LTGs is desirable, not just because they are rare, but also because they are good laboratories for exploring the behaviour of radio jets in disc environments. While this is relatively rare at low redshift, the connection between black holes and discs is likely to have been a common feature of galaxy evolution around the peak epoch of star formation ($z \sim 2$) when most of today’s stellar mass was created. Radio AGN in LTGs may therefore hold clues to the interplay between AGN and star formation at these critical epochs. Our main results are as follows.

- (i) The radio AGN in LTGs are predominantly found in galaxies that have high stellar masses ($M_* > 10^{10.8} M_\odot$), red colours and low

³ Note that the well-known misalignment of kpc-scale radio jets with the galaxy disc (Ulvestad & Wilson 1984) does not pose a serious problem to this interpretation, since parsec and kpc-scale radio jets are often spectacularly misaligned, as illustrated in Cen A (Israel 1998; Feain et al. 2009).

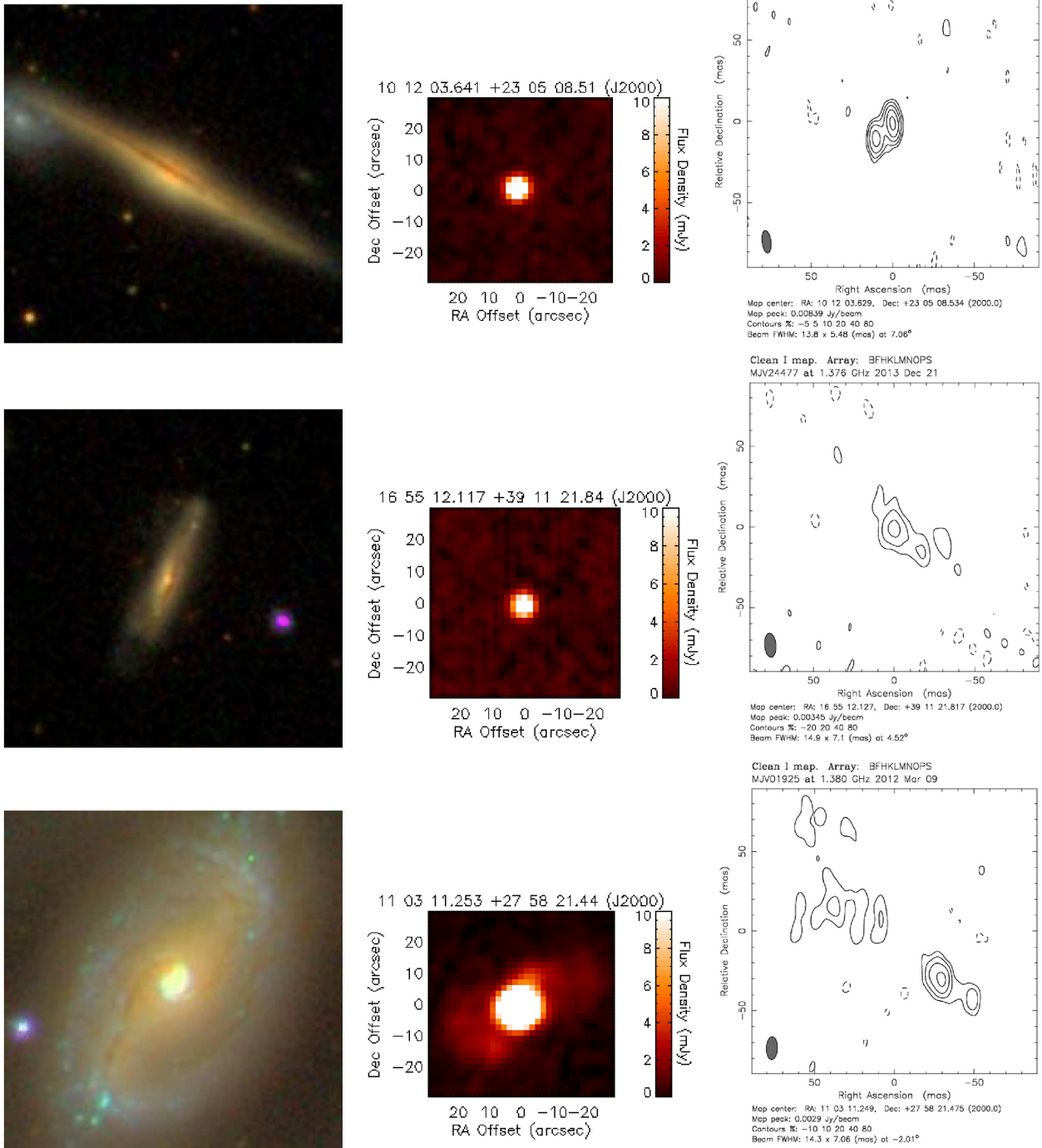


Figure 8. SDSS (left), FIRST (middle) and mJIVE-20 (right) images of three spiral AGN hosts in our sample, that are close to edge-on with evidence for a jet in the VLBI image. Note that, in the last example (bottom row), the jet is shown slightly off centre, in order to capture all of the structure around this galaxy on the same spatial scales as for the other two galaxies.

star formation rates, with a negligible dependence on the detailed morphology or local environment of the host galaxy.

(ii) A high fraction (~ 50 per cent) of spiral AGN hosts exhibit morphological disturbances that are indicative of recent mergers. The merger fraction is around a factor of 4 higher than that in the general LTG population, indicating that mergers are likely to be an important trigger for the radio AGN in these systems.

(iii) The fraction of LTG AGN hosts that reside on the red sequence is almost a factor of 2 higher than that in the general LTG population. In a similar vein to what has been suggested in the recent literature, the pre-dominantly red colours of the LTG AGN hosts suggest that the triggering of radio AGN in these systems is generally delayed with respect to the peak of the associated star formation episode, reducing the AGN's ability to regulate the stellar

mass growth. Together with the recent literature, it seems reasonable to suggest that in starbursts where the gas is accreted via a merger in the nearby Universe, AGN feedback is unlikely to strongly regulate the resultant star formation.

(iv) In LTGs that exhibit parsec-scale jets in the VLBI images, we find that the orientations of these jets appear to be roughly perpendicular to the major axis of the host galaxy. If the black holes and discs co-evolve in these systems, then one might expect the black hole spin axes to align with the stellar discs which, in turn, would produce the observed alignment between the galaxy disc and the jet.

ACKNOWLEDGEMENTS

We thank the referee, Elaine Sadler, for many constructive comments that allowed us to improve the quality of the original manuscript. We are grateful to Martin Hardcastle for many interesting discussions. We thank Meg Urry and Kevin Schawinski for useful comments. SK is grateful for support from the University of Tasmania (UTas) via a UTas Visiting Scholarship and acknowledges a Senior Research Fellowship from Worcester College Oxford. SSS acknowledges an ARC Early-Career Fellowship (DE130101399). ATD was supported by an NWO Veni Fellowship.

REFERENCES

- Abazajian K. N. et al., 2009, *ApJS*, 182, 543
 Baan W. A., 2007, in Chapman J. M., Baan W. A., eds, *Proc. IAU Symp. 242 Astrophysical Masers and their Environments*. Cambridge Univ. Press, Cambridge, p. 437
 Bagchi J. et al., 2014, *ApJ*, 788, 174
 Baldwin J. A., Phillips M. M., Terlevich R., 1981, *PASP*, 93, 5
 Barnes J. E., Hernquist L., 1992, *ARA&A*, 30, 705
 Best P. N., Heckman T. M., 2012, *MNRAS*, 421, 1569
 Binney J., Tremaine S., 1987, *Princeton Series in Astrophysics: Galactic Dynamics*, 1st edn. Princeton Univ. Press, Princeton, NJ
 Blandford R. D., Znajek R. L., 1977, *MNRAS*, 179, 433
 Blanton M. R., Roweis S., 2007, *AJ*, 133, 734
 Brinchmann J., Charlot S., White S. D. M., Tremonti C., Kauffmann G., Heckman T., Brinkmann J., 2004, *MNRAS*, 351, 1151
 Carpineti A., Kaviraj S., Darg D., Lintott C., Schawinski K., Shabala S., 2012, *MNRAS*, p. 2262
 Cattaneo A. et al., 2009, *Nature*, 460, 213
 Chiaberge M., Marconi A., 2011, *MNRAS*, 416, 917
 Croton D. J. et al., 2006, *MNRAS*, 365, 11
 Davies R. I., Maciejewski W., Hicks E. K. S., Tacconi L. J., Genzel R., Engel H., 2009, *ApJ*, 702, 114
 de Vaucouleurs G., 1959, *Handbuch Phys.*, 53, 275
 Deller A. T., Middelberg E., 2014, *AJ*, 147, 14
 Edelson R. A., 1987, *ApJ*, 313, 651
 Ekers R. D., Goss W. M., Kotanyi C. G., Skellern D. J., 1978, *A&A*, 69, L21
 Ellison S. L., Patton D. R., Mendel J. T., Scudder J. M., 2011, *MNRAS*, 418, 2043
 Englmaier P., Shlosman I., 2000, *ApJ*, 528, 677
 Fabian A. C., 2012, *ARA&A*, 50, 455
 Feain I. J. et al., 2009, *ApJ*, 707, 114
 Gammie C. F., Goodman J., Ogilvie G. I., 2000, *MNRAS*, 318, 1005
 Gliozzi M., Papadakis I. E., Grupe D., Brinkmann W. P., Raeth C., Kedziora-Chudczer L., 2010, *ApJ*, 717, 1243
 Greene J. E. et al., 2013, *ApJ*, 771, 121
 Gültekin K. et al., 2009, *ApJ*, 698, 198
 Hardcastle M. J., Evans D. A., Croston J. H., 2007, *MNRAS*, 376, 1849
 Hatton S., Devriendt J. E. G., Ninin S., Bouchet F. R., Guiderdoni B., Vibert D., 2003, *MNRAS*, 343, 75
 Hopkins A. M., Beacom J. F., 2006, *ApJ*, 651, 142
 Hopkins P. F., Quataert E., 2010, *MNRAS*, 407, 1529
 Hubble E. P., 1926, *ApJ*, 64, 321
 Inskip K. J., Tadhunter C. N., Morganti R., Holt J., Ramos Almeida C., Dicken D., 2010, *MNRAS*, 407, 1739
 Israel F. P., 1998, *A&AR*, 8, 237
 Iwasawa K., Sanders D. B., Evans A. S., Trentham N., Miniutti G., Spoon H. W. W., 2005, *MNRAS*, 357, 565
 Kauffmann G. et al., 2003, *MNRAS*, 341, 33
 Kaviraj S., 2009, *MNRAS*, 394, 1167
 Kaviraj S., 2010, *MNRAS*, 406, 382
 Kaviraj S., 2014, *MNRAS*, 440, 2944
 Kaviraj S., Tan K.-M., Ellis R. S., Silk J., 2011, *MNRAS*, 411, 2148
 Kaviraj S. et al., 2013, *MNRAS*, 429, L40
 Kaviraj S., Shabala S. S., Deller A. T., Middelberg E., 2015, *MNRAS*, 452, 774
 Keel W. C., White R. E., III, Owen F. N., Ledlow M. J., 2006, *AJ*, 132, 2233
 Kewley L. J., Groves B., Kauffmann G., Heckman T., 2006, *MNRAS*, 372, 961
 Kim W.-T., Seo W.-Y., Kim Y., 2012, *ApJ*, 758, 14
 Kocevski D. D. et al., 2012, *ApJ*, 744, 148
 Komatsu E. et al., 2011, *ApJS*, 192, 18
 Koss M., Mushotzky R., Veilleux S., Winter L., 2010, *ApJ*, 716, L125
 Ledlow M. J., Owen F. N., Keel W. C., 1998, *ApJ*, 495, 227
 Ledlow M. J., Owen F. N., Yun M. S., Hill J. M., 2001, *ApJ*, 552, 120
 Lonsdale C. J., Diamond P. J., Thrall H., Smith H. E., Lonsdale C. J., 2006, *ApJ*, 647, 185
 Maciejewski W., Teuben P. J., Sparke L. S., Stone J. M., 2002, *MNRAS*, 329, 502
 McKinney J. C., Tchekhovskoy A., Blandford R. D., 2013, *Science*, 339, 49
 McNamara B. R., Nulsen P. E. J., 2007, *ARA&A*, 45, 117
 Madau P., Pozzetti L., Dickinson M., 1998, *ApJ*, 498, 106
 Maloney P. R., Begelman M. C., Pringle J. E., 1996, *ApJ*, 472, 582
 Mao M. Y., Norris R. P., Emonts B., Sharp R., Feain I., Chow K., Lenc E., Stevens J., 2014, *MNRAS*, 440L, 31
 Martini P., Regan M. W., Mulchaey J. S., Pogge R. W., 2003, *ApJ*, 589, 774
 Morganti R., Oosterloo T. A., Tadhunter C. N., van Moorsel G., Killeen N., Wills K. A., 2001, *MNRAS*, 323, 331
 Norris R. P., Allen D. A., Roche P. F., 1988, *MNRAS*, 234, 773
 Norris R. P., Kesteven M. J., Troup E. R., Allen D. A., Sramek R. A., 1990, *ApJ*, 359, 291
 Norris R. P., Lenc E., Roy A. L., Spoon H., 2012, *MNRAS*, 422, 1453
 Oke J. B., Gunn J. E., 1983, *ApJ*, 266, 713
 Phillips R. B., Mutel R. L., 1982, *A&A*, 106, 21
 Pringle J. E., 1997, *MNRAS*, 292, 136
 Sadler E. M., Slee O. B., Reynolds J. E., Roy A. L., 1995, *MNRAS*, 276, 1373
 Sadler E. M., Ekers R. D., Mahony E. K., Mauch T., Murphy T., 2014, *MNRAS*, 438, 796
 Sanders D. B., Soifer B. T., Elias J. H., Madore B. F., Matthews K., Neugebauer G., Scoville N. Z., 1988, *ApJ*, 325, 74
 Sarzi M. et al., 2010, *MNRAS*, 402, 2187
 Schawinski K., Thomas D., Sarzi M., Maraston C., Kaviraj S., Joo S.-J., Yi S. K., Silk J., 2007, *MNRAS*, 382, 1415
 Schawinski K., Simmons B. D., Urry C. M., Treister E., Glikman E., 2012, *MNRAS*, 425, L61
 Scott C., Kaviraj S., 2014, *MNRAS*, 437, 2137
 Shabala S. S., Ash S., Alexander P., Riley J. M., 2008, *MNRAS*, 388, 625
 Shabala S. S. et al., 2012, *MNRAS*, 423, 59
 Sikora M., Stawarz Ł., Lasota J.-P., 2007, *ApJ*, 658, 815
 Somerville R. S., Gilmore R. C., Primack J. R., Domínguez A., 2012, *MNRAS*, 423, 1992
 Springel V., Di Matteo T., Hernquist L., 2005, *MNRAS*, 361, 776

- Strateva I. et al., 2001, *AJ*, 122, 1861
Tabor G., Binney J., 1993, *MNRAS*, 263, 323
Tremonti C. A. et al., 2004, *ApJ*, 613, 898
Ulvestad J. S., Wilson A. S., 1984, *ApJ*, 285, 439
van Dokkum P. G., 2005, *AJ*, 130, 2647
Veilleux S., Osterbrock D. E., 1987, *ApJS*, 63, 295
Weiler K. W., Williams C. L., Panagia N., Stockdale C. J., Kelley M. T.,
Sramek R. A., Van Dyk S. D., Marcaide J. M., 2007, *ApJ*, 671, 1959
Wild V., Heckman T., Charlot S., 2010, *MNRAS*, 405, 933
Wilkinson P. N., Polatidis A. G., Readhead A. C. S., Xu W., Pearson T. J.,
1994, *ApJ*, 432, L87
- Wilson A. S., Colbert E. J. M., 1995, *ApJ*, 438, 62
Yang X., Mo H. J., van den Bosch F. C., Pasquali A., Li C., Barden M.,
2007, *ApJ*, 671, 153
Yuan W., Zhou H. Y., Komossa S., Dong X. B., Wang T. G., Lu H. L., Bai
J. M., 2008, *ApJ*, 685, 801
Zhou H. et al., 2007, *ApJ*, 658, L13

This paper has been typeset from a $\text{\TeX}/\text{\LaTeX}$ file prepared by the author.